International Journal of Heat and Technology
Vol. 40, No. 1, February, 2022, pp. 137-144
Journal homepage: http://iieta.org/journals/ijht

Effect of Surface Motion on Heat Transfer and Pressure Force from Multiple Impinging Jets– A Numerical Study

Ali Chitsazan[1*], Georg Klepp[1], Birgit Glasmacher[2]

[1] Institute for Energy Research, Ostwestfalen-Lippe University of Applied Sciences and Arts, Lemgo 32657, Germany
[2] Institute for Multiphase Processes, Leibniz University Hannover, Hannover 30167, Germany

Corresponding Author Email: ali.chitsazan@yahoo.com

https://doi.org/10.18280/ijht.400116

Received: 22 October 2020
Accepted: 8 November 2021

Keywords:
multiple jet, heat transfer, pressure force, surface motion, angled jet, jet arrangement

ABSTRACT

The effect of jet arrangement, jet Re number, jet exit angle (θ), the nozzle-to-surface distance (H/d), jet-to-jet spacing (S/d) on the heat transfer, and pressure force performance from multiple impinging round jets on a moving flat surface have been numerically evaluated. There is a minor difference between in-line and staggered arrangements on a moving flat surface. The averaged Nusselt number on a moving flat surface reduces with an increase in the relative velocity (VR). The surface motion effects become more pronounced on the local Nu distribution at low Re, small S/d, large H/d, and angled jets for a moving flat surface. The pressure force coefficient on a moving flat surface is highly dependent on the H/d and θ but relatively insensitive to the VR, Re, and S/d within the range examined. Two correlations are developed and validated for the average Nu and force coefficient and the agreement between the CFD and correlation is found to be reasonable.

1. INTRODUCTION

Multiple impinging jets have many applications in industry such as heating, cooling, and drying. A review of the heat transfer and flow phenomena from the multiple impinging jets is presented by Weigand et al. [1, 2]. With decreased H/d or S/d, the jet interaction increases significantly [1, 2]. Lee et al. [3] found that the cross-flow decreases the jet impingement heat transfer. Katti et al. [4] stated that the jet impingement heat transfer decreases for the small S//d and large H/d. San et al. [5] stated that the jet interference before impingement on the target surface decreases the heat transfer rate. Li et al. [6] investigated the parallel multiple jets flow and heat transfer. The heat transfer characteristics have a high dependency on the Re, S/d, and H/d. Chandramohan et al. [7] observed that the Re and H/d have a significant contribution to the jet impingement heat transfer.

Li et al. [8] found that the jet inclination has a minor influence on the jet impingement heat transfer within the error margin. Li et al. [9] found that two flow regimes are depending on the H/d and the heat transfer rate for inclined and orthogonal jets was similar. Ekkad et al. [10] stated that the heat transfer rate at the stagnation point for a normal jet is higher than the angled jet. Kamal et al. [11] stated that the uniform pressure distribution along the target surface and largest drying rate were achieved for S/d = 3.5, H/d=6, and θ= 60°. Attala et al. [12] found that the maximum heat transfer rate occurs for a jet inclination between 10° and 20°.

Chattopadhyay [13] stated that the surface motion reduces the heat transfer rate. Badra et al. [14] investigated the transient jet impingement heat transfer on a moving surface numerically. Kadiyala and Chattopadhyay [15] found that the maximum jet impingement heat transfer rate on a moving flat surface is achieved at a VR equal to 6.

Xing et al. [16] stated that if there is no dependency on cross-flow or H/d, the in-line pattern performs better than the staggered pattern. Wae-Hayee et al. [17] found that the average Nu of the in-line pattern is approximately 13-20% higher than that of the staggered pattern.

Wang et al. [18] stated that the jet force coefficient for a single jet has a high dependency on the H/d and is relatively insensitive to the Re. Peter et al. [19] found that decreasing the θ decreases the total force from the radial jets.

Direct numerical simulation (DNS) is still limited to a single jet or small Re [20]. Large eddy simulation (LES) is computationally expensive [21]. The Reynolds-averaged Navier-Stokes equations with an appropriate turbulence model such as the SST k-omega model are computationally less expensive [14, 15].

Data for multiple impinging jets on a moving flat surface with varying the jet arrangement, θ, jet velocity, and surface velocity to provide the best configuration for the heat transfer rate and the jet impingement force is rare in the literature. The objective of this research is to investigate the effect of the nozzle arrangement, the Re, H/d, S/d, θ, and the surface motion on the jet impingement heat transfer and pressure force on a moving flat surface numerically for an optimum design of the industrial drying application.

2. MATERIAL AND METHOD

2.1 Definition of characteristic numbers

The Nu is defined by the following expression:

$$Nu = \frac{hd}{k} = \frac{q}{(T_w - T_j)} \cdot \frac{d}{k} \quad (1)$$

where, h is the local heat transfer coefficient, d is the nozzle diameter, k is the thermal conductivity, q is the convective heat flux, T_w is the surface temperature, and T_j is the jet temperature.

Pressure force on the surface is the force that the fluid exerts normally to the surface. Pressure force on the impingement surface is presented in dimensionless form by a force coefficient C_f. The force coefficient of a surface is defined as follows:

$$Cf = \frac{F}{0.5\rho V^2(\pi d^2/4)} \quad (2)$$

where, F is the pressure force on the surface, ρ is the jet density, d is the nozzle diameter and V is the jet exit velocity. The pressure force on the surface is computed as:

$$Ff = P_{st}A \quad (3)$$

where, P_{st} is the pressure at the stagnation point and A is the area of the target surface.

2.2 Domain and boundary condition

Figure 1 shows the geometry and the boundary conditions. The jet flow is assumed to be with a uniform temperature and velocity profile. The target surface as a moving flat surface was modeled as a no-slip wall at a constant temperature of T_w=60°C. No-slip with adiabatic wall boundary condition is applied on all other solid surfaces. Constant pressure outlet boundary condition is applied for outlets. A symmetric boundary condition was also applied in the X-Y plane.

The investigated parameters are presented in Table 1. The investigated parameters include the Re, H/d, S/d, θ, and the VR i.e., ratio of surface velocity to jet velocity. The jet exit diameter, the jet temperature, and the surface temperature are maintained constant.

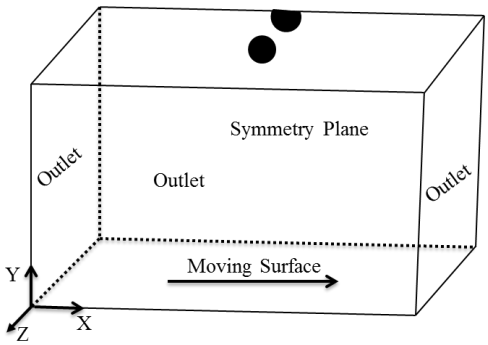

Figure 1. Schematic of the computational domain

Table 1. Investigated parameters for a real industrial dryer

Parameters	Values
Number of jet rows	1
Number of jets in a row	3
Re	1980, 10000, 23000, 40000, 66200
H/d	1, 2, 5, 10, 15, 20
S/d	2, 4, 6, 10
θ	45, 60, 90 (deg)
VR	0, 0.048, 0.28, 0.5, 1
Surface temperature	60°C
Inlet Jet temperature	25°C

2.3 Computational detail

The commercial code STAR-CCM$^+$ is used to build up the numerical setup [22]. The SIMPLE algorithm, the second-order discretization upwind scheme, and the SST k-ω turbulence model were applied [14, 15]. The flow in the proximity of the wall is simulated with the low-Reynolds number implementation. An unstructured polyhedral grid was generated by the STAR-CCM$^+$. The grid convergence index method (GCI) is applied for a grid sensitivity study [23]. The solution is converged if the scaled residual of all governing equations is less than 10^{-4}.

3. RESULTS AND DISCUSSION

3.1 Evaluation of computational model

Figure 2 indicates the average Nu on the moving flat surface. Due to the absence of experimental data, the numerical results from this work have been compared with a numerical investigation conducted by Chattopadhyay [13]. They chose the realizable k-ε model for simulation. Here the values of averaged Nu are presented at different relative velocities and varied up to 1.0. This reveals a good agreement between the literature and CFD data from this work. The slope and trend of the numerical results are in agreement with the literature. The difference between the data from literature and the CFD data from this work is approximately 14% on average and the SST turbulence model represents a reasonable accuracy. Differences in the turbulence model (realizable k-ε and SST K-ω), thermal boundary condition at target surface (due to the unknown boundary condition in the literature), and software (FLUENT and STAR-CCM$^+$) influence the comparison.

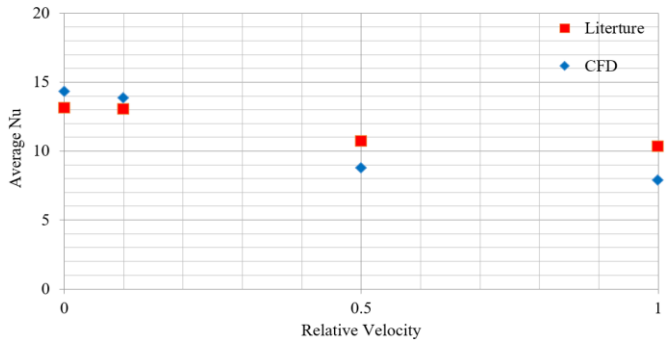

Figure 2. Comparison between average Nu from literature and CFD (H/d=2, S/d=10, θ=90°, Re=2500)

3.2 Jet arrangement

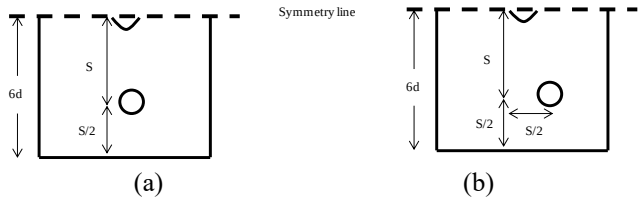

Figure 3. Sketch of jet arrangement: (a) In-line arrangement and (b) staggered arrangement

The arrays of jet arrangements as the in-line arrangement in (a) and the staggered arrangement in (b) are shown in Figure

3. The diameter *d* of each round orifice through a confinement plate of 120 mm length is 10 mm. Both jet arrangements have the same array of one row with three jet holes with *S*=4*d* and H=5*d*. Because of symmetry, only half of the confinement surface is presented.

The contours of the local Nu on the moving flat surface for the in-line and staggered arrangements are shown in Figure 4. It can be concluded from the literature for a fixed flat surface [16, 17] that the jets are protected from the cross-flow for the in-line arrangement. The cross-flow influences the jets more directly for the staggered arrangement which causes stronger diffusion and reduces the heat transfer rate. This trend can be observed for a moving flat surface (see Figures 4 and 5). However, there is a minor difference between the in-line and staggered arrangement on the moving flat surface (see Figure 5). The in-line arrangement has a more uniform heat transfer distribution compared to the staggered arrangement. In the following, the in-line arrangement is considered for further investigation.

3.3 Surface motion

3.3.1 Effect on heat transfer

Figure 6 compares the effect of the VR defined as the surface velocity to the jet velocity (VR) equal to 0, 0.0047 (surface velocity=0.17), 0.047(surface velocity=1.7), and 0.28 (surface velocity=10) on the averaged Nu on the moving flat surface. The surface motion has a minor effect on the total averaged Nu for a small VR (0.0047 and 0.047).

It can be seen that the total averaged Nu reduces with an increase in the VR. The Nu distribution is influenced by the jet which is entrained by the moving surface. This influence becomes more pronounced as the VR increases (see Figure 7). Thus, the surface motion reduces the effectiveness of each impingement jet.

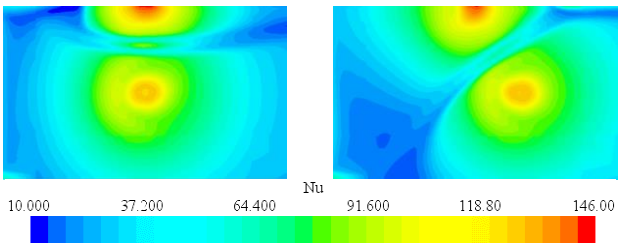

(a) In-line Arrangement (b) Staggered Arrangement

Figure 4. Nu distributions for Re=23000, S/d=4, H/d=5, θ=90°, VR=0.28

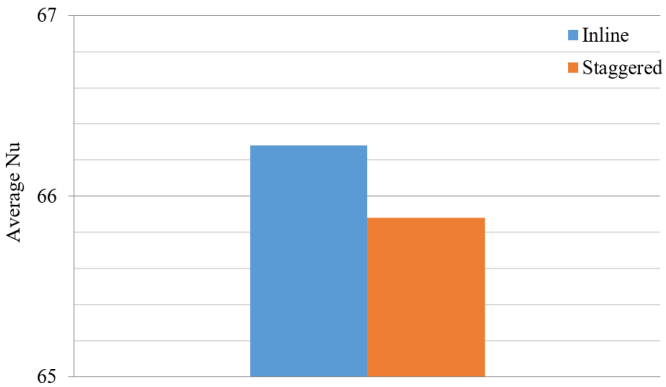

Figure 5. Comparison of average Nu for different nozzle arrangements (S/d=4, H/d=5, Re=23000, θ=90°, VR=0.28)

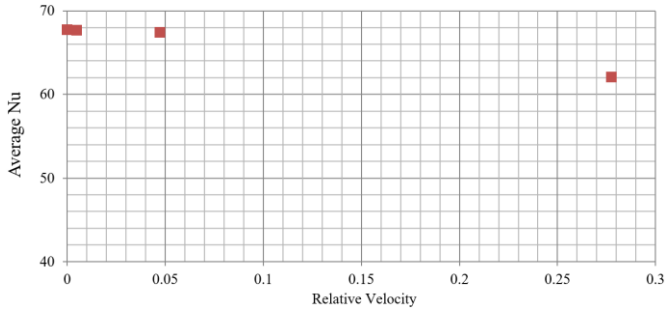

Figure 6. Effects of VR on the average Nu (S/d=4, H/d=2, θ=90°, Re=23000)

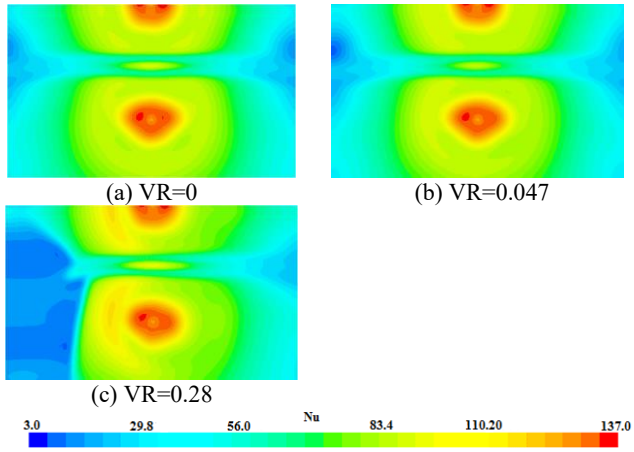

Figure 7. Nu distribution on a moving flat surface for different VR (H/d=2, Re=23000, θ=90°, S/d=4)

Due to the moving surface, the impinging jet is entrained resulting in slightly reduced heat transfer coefficients. Nevertheless, for a moving surface with surface velocities significantly smaller than the jet velocity the impinging jet is still the predominant phenomenon.

3.3.2 Effect on pressure force

Figure 8 compares the effect of the VR on the pressure force coefficient on the moving flat surface. When the VR increases, the pressure force coefficient on the moving flat surface reduces slightly due to the decrease in pressure on the moving flat surface. However, the pressure force is relatively insensitive to the VR on the moving flat surface.

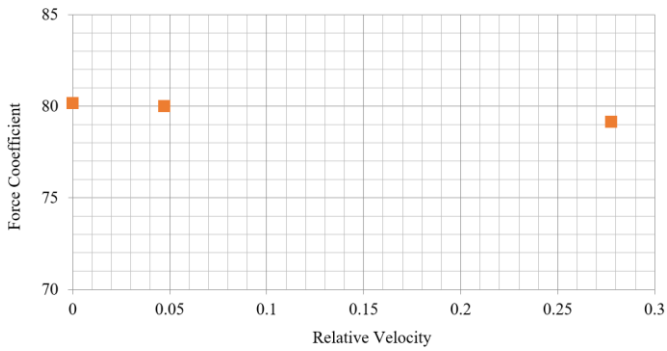

Figure 8. Effects of VR on the pressure force coefficient (H/d=2, S/d=4, θ=90°, Re=23000)

3.4 Jet Reynolds number (Re)

3.4.1 Effect on heat transfer

Figure 9 compares the effect of the Re on the average Nu.

The results show that the average Nu increases as the Re increases from 1980 to 66200. A higher Re corresponds to a higher jet velocity and the strong flow acceleration associated with the higher jet velocities contributes greatly to enhance the heat transfer rate (see Figure 10).

Due to the surface velocity (VR=0.28), the impinging jet is entrained in the direction of the surface motion. The resulting uneven distribution slightly reduces the overall heat transfer. With increasing Re there is a more uniform distribution of the heat transfer (see Figure 10). Thus, the influence of the moving surface and the entrainment is also less for a higher Re.

A high Re correlates with a desirable high heat transfer rate but also often with high undesirable energy consumption. Including the additional design parameters, should help to find an optimum solution.

3.4.2 Effect on pressure force

Figure 11 compares the effect of jet Re on the pressure force coefficient. Increasing the Re occurs with increasing the jet velocity. Due to the definition of the pressure force coefficient on the target surface (see Eq. (2)), the pressure force coefficient is relatively insensitive to the jet Re. This result correlates with the findings of Wang et al. [18].

3.5 Nozzle-to-surface distance (*H/d*)

3.5.1 Effect on heat transfer

Figure 12 compares the effect of the H/d on the average N. The results show that the average Nu varies quite strongly with *H/d* and the average Nu increases as *H/d* decreases.

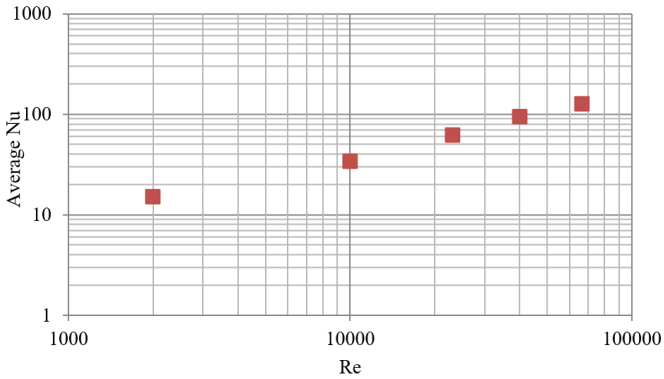

Figure 9. Effects of Re on the average Nu in logarithmic scale (S/d=4, H/d=2, θ=90°, VR=0.28)

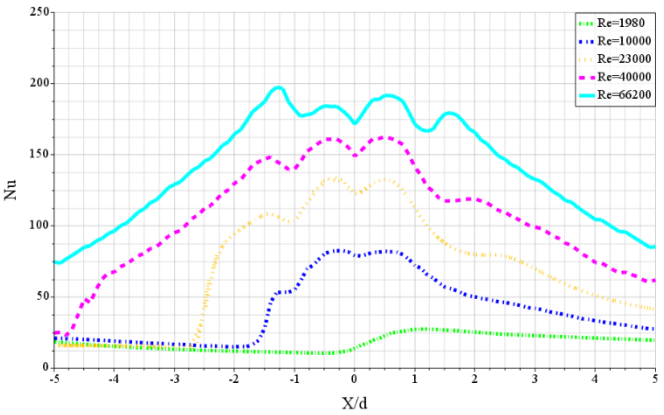

Figure 10. Effects of Re on the local Nu along motion direction (S/d=4, H/d=2, θ=90°, VR=0.28)

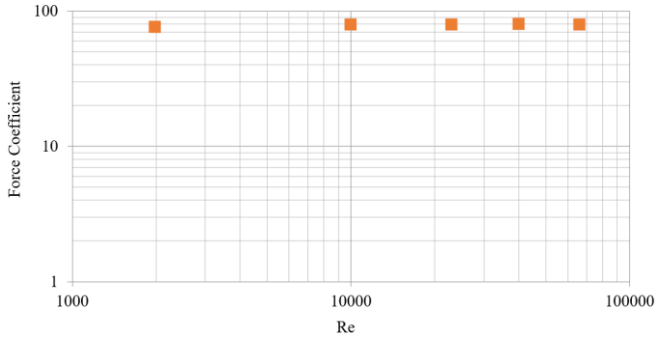

Figure 11. Effects of Re on the pressure force coefficient (S/d=4, H/d=2, θ=90°, VR=0.28)

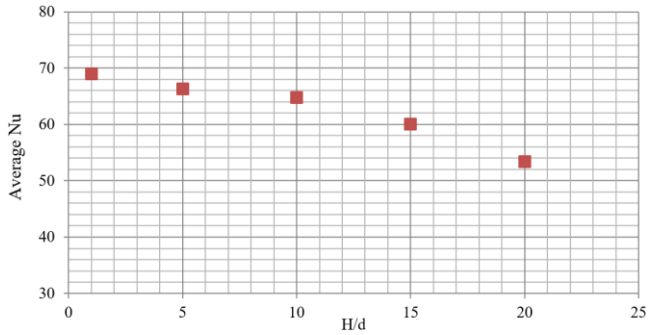

Figure 12. Effects of the H/d on the average Nu (*S/d*=4, Re=23000, θ=90°, VR=0.28)

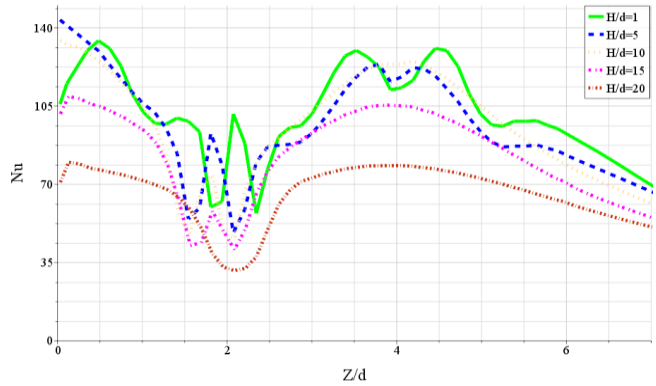

Figure 13. Effect of the H/d on the local Nu (S/d=4, Re=23000, θ=90°, VR=0.28)

The interference of adjacent jets before impingement degrades the heat transfer in the stagnation region, whereas the interactions of the surface jets at the wall (impingement surface) increase the heat transfer. With increasing H/d the interference of the adjacent jets increases and the jet interaction on the wall surface decreases, causing a smaller and more evenly distributed heat transfer (see Figure 13).

The effect of the surface motion on the heat transfer is strongly influenced by the H/d (see Figure 14). The effect of the surface motion on the heat transfer is less distinct for higher H/d (15 and 20). For lower H/d (H/d = 5 and 10) there is a distinct minimum in the heat transfer distribution. For very low H/d (H/d =1) the flow is mainly influenced by the confinement between the upper plate and target surface and the influence of the entrainment by the moving surface is negligible.

Minimizing the H/d as much as possible and taking into account the other effects (see the effect on pressure force) seems a good approach for an efficient process.

3.5.2 Effect on pressure force

Figure 15 compares the effect of the H/d on the pressure force coefficient. Results indicate that the pressure force coefficients on the target surface have a high dependency on the H/d.

The pressure force coefficients increase with decreasing the H/d as the momentum exchange between the jet flow and the ambient leads to the increase in the pressure on the impingement surface. Therefore, the identification of an optimum H/d is very important for the processing of products sensitive to pressure forces, such as paper. This result correlates with the findings of Wang et al. [18].

3.6 Jet-to-jet spacing (S/d)

3.6.1 Effect on heat transfer

Sketches of the different configurations with the in-line arrangement and different S/d are shown in Figure 16. The diameter of each round orifice (d) through a confinement plate with the constant length 14d is 10 mm. All configurations have the same array of 1 row with different S/d over the range of S=2d-10d and H=2d. The area used for computing the average heat transfer coefficient remains the same for all four cases.

Figure 17 compares the effect of the S/d on the average Nu. The averaged Nu sharply decreases with a decrease in the S/d. The minimum Nu is found in the lower S/d = 2 compared to the other cases.

The wall jet flows are impinging upon each other and forming a new stagnation region. This wall jet interaction is more distinct for the lower S/d (see Figure 18).

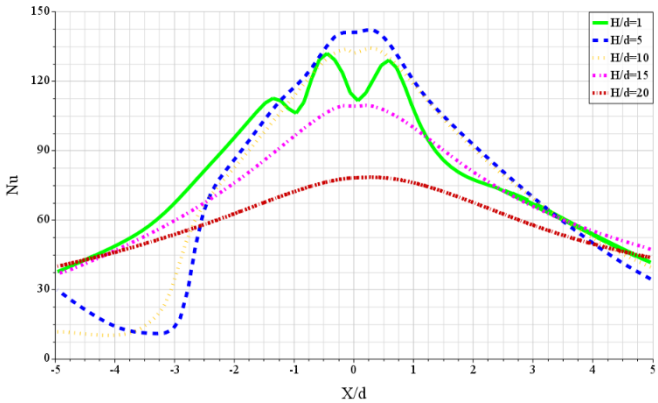

Figure 14. Effect of the H/d on local Nu along motion direction (S/d=4, Re=23000, θ=90°, VR=0.28)

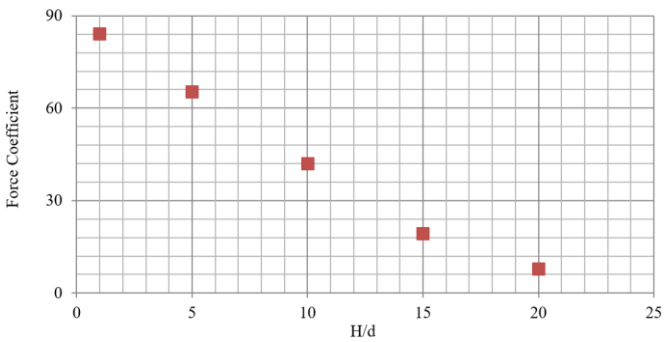

Figure 15. Effect of the H/d on the pressure force coefficient (S/d=4, Re=23000, θ=90°, VR=0.28)

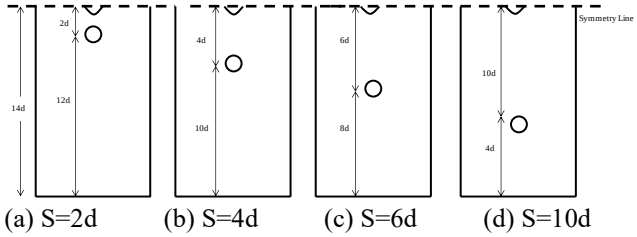

Figure 16. Sketch of the different S/d

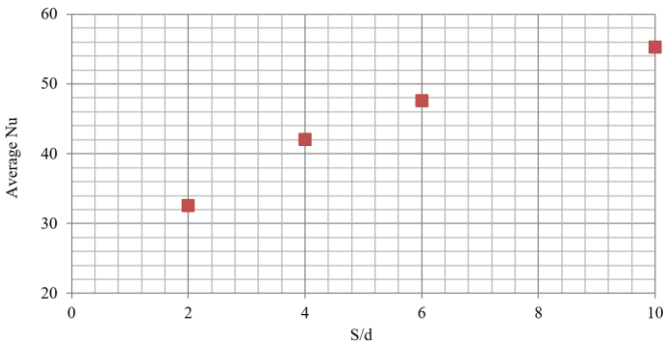

Figure 17. Effect of the S/d on the average Nu (H/d=2, Re=23000, θ=90°, VR=0.28)

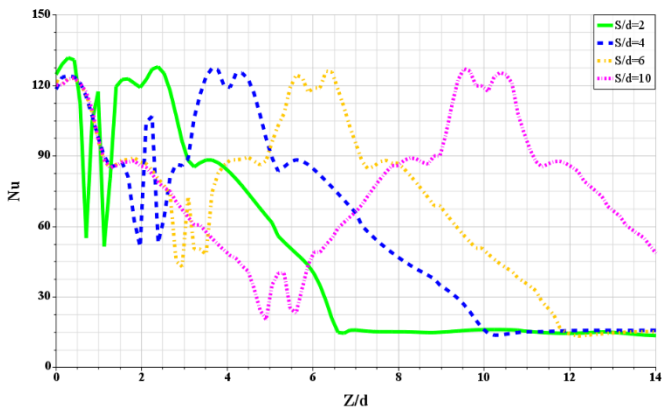

Figure 18. Effects of the S/d on the local Nu (H/d=2, Re=23000, θ=90°, VR=0.28)

With increasing the S/d from the impingement zone, the heat transfer strongly decreases as the S/d decreases. For the high values of the S/d in this analysis, the jets are more evenly distributed over the area thus leading to higher average Nu.

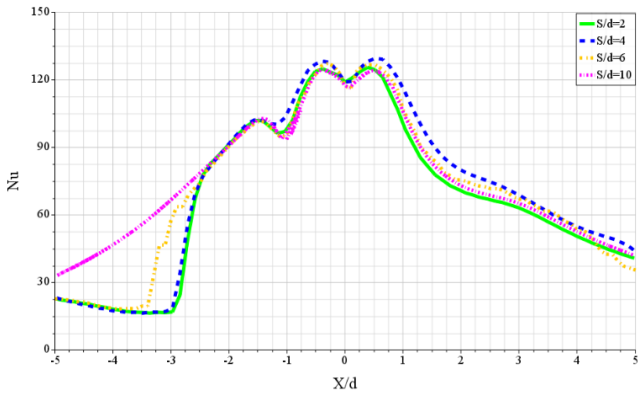

Figure 19. Effect of the S/d on local Nu along motion direction at Z=0 (H/d=2, Re=23000, θ=90°, VR=0.28)

The surface motion has more effect on the heat transfer distribution at lower values of the S/d and the heat transfer is more uniform for jets at high *S/d* values, (see Figure 19). Thus, an optimum for the heat transfer might be achieved for a uniform distribution of the jet orifices.

3.6.2 Effect on pressure force

Figure 20 compares the effect of the S/d on the pressure force coefficient. Results indicate that the pressure force coefficient is relatively insensitive to the S/d within the range examined.

3.7 Jet exit angle (θ)

3.7.1 Effect on heat transfer

Figure 21 shows the variation of the averaged Nu with the θ for small H/d=1. The θ is varied between 45°, 60°, and 90° as measured with respect to the horizontal axes. The averaged Nu for the angled jets is significantly lower than for the orthogonal jet. The angled jets cause an asymmetric distribution of the heat transfer: The decrease on the side with the lower flow is much stronger than the increase on the side with the higher flow thus leading to a decrease in the averaged heat transfer with decreasing the θ, (see Figure 22).

Figure 22 shows the computed Nu distribution in the motion direction (left to right) for various θ. The flow is influenced by the θ, the movement of the impingement surface, and the confinement between the upper plate and the moving surface. The primary and the secondary peaks are observed in the Nu distribution of orthogonal impinging jets in contrast to the angled jets. The Nu at the stagnation point shows no significant change for angled jets and is higher than the orthogonal jet with shifted locations of the peak values. The Nu for angled jets on the right side of the impingement surface is much larger than that on the left side. Because the angled jet leads to the main flow toward the right side of the impingement surface, and the jet flow toward the left side will be confined. Therefore, the Nu curves for angled jets exhibit a more asymmetrical trend compared to the Nu curves for orthogonal jets.

For practical applications, the orthogonal jet is preferable to angled jets, at least for low H/d.

3.7.2 Effect on pressure force

Figure 23 compares the effect of the θ on the pressure force coefficient. The pressure force coefficient is highly dependent on the θ and increases with increasing the θ. The pressure force coefficient correlates strongly with the normal component of the jet flow. Decreasing the θ, the normal component of the jet flow decreases but the parallel component to the surface increases having a negative effect. Hence, an orthogonal jet (90°) can exert the most pressure upon impinging the surface.

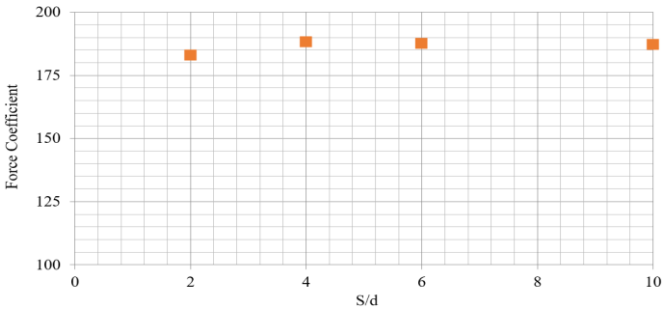

Figure 20. Effect of the S/d on the pressure force coefficient (H/d=2, Re=23000, θ=90°, VR=0.28)

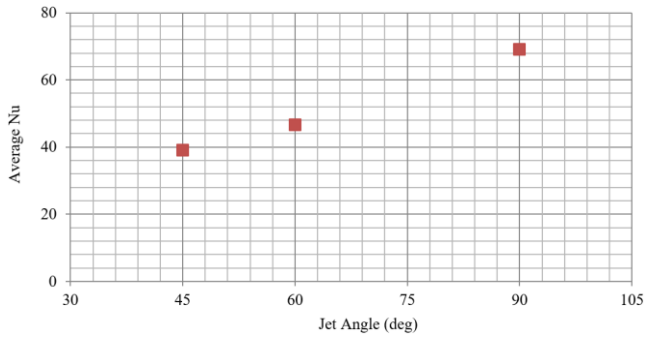

Figure 21. Effects of θ on the average Nu (H/d=1, Re=23000, S/d=4, θ=90°, VR=0.28)

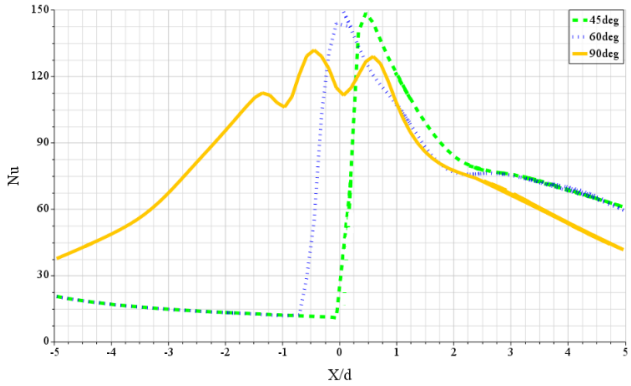

Figure 22. Effects of the θ on local Nu along motion direction (H/d=1, Re=23000, S/d=4, θ=90°, VR=0.28)

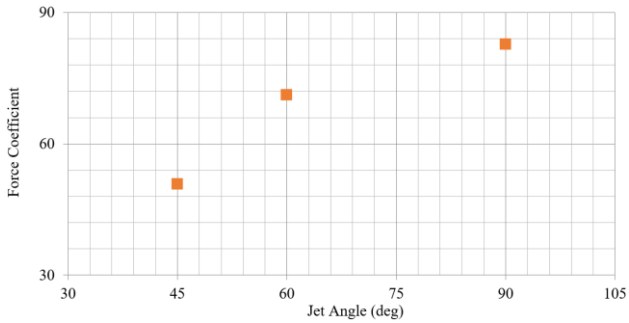

Figure 23. Effects of the θ on the pressure force coefficient (H/d=1, Re=23000, *S/d*=4, θ=90°, VR=0.28)

3.8 Correlation equations

A correlation for the averaged Nu and a correlation for the pressure force coefficient is developed by a multiple regression fit:

$$Nu_{ave} = 0.082\,\mathrm{Re}^{0.6}(H/d)^{-0.054}(S/d)^{0.2}\theta_{rad}^{0.84}(1+VR)^{-0.027} \quad (4)$$

$$C_f = 0.7\,\mathrm{Re}^{0.013}(135H/d^{-0.096} - 2.5H/d - 44.93)\,(S/d)^{-0.0041}\theta_{rad}^{0.61}(1+2.6VR)^{-0.03} \quad (5)$$

The above correlations are proposed in terms of the independent parameters for Re between 1980 and 66200, H/d between 1 and 20, S/d between 2 and 10, θ between 45 and 90°, and VR between 0 and 0.28. The deviation between the numerical simulation and correlation equations was reasonable and by less than 5% for the averaged Nu as well as for the pressure force coefficient.

4. CONCLUSION

The effect of the jet arrangement, VR, Re, θ, H/d, and S/d on the heat transfer and pressure force performance have been evaluated. The results are as follows:

- There is a minor difference between inline and staggered arrangements on a moving flat surface. The inline arrangement has a more uniform heat transfer distribution compared to the staggered arrangement.
- The averaged Nu on a moving flat surface reduces with an increase in the VR.
- The surface motion effects become more pronounced on the Nu distribution as the Re decreases. The results show that the average Nu on a moving flat surface increases as Re increases. The dependencies are of the same order of magnitude as for the static surface.
- The surface motion has a greater effect on the Nu distribution at the low H/d. and the transfer coefficients are more evenly distributed for jets at the high H/d. The results show that the averaged Nu increases as the H/d decreases.
- The surface motion has a greater effect on the Nu distribution on a moving flat surface at the low S/d and the transfer coefficients are more uniformly distributed for big S/d between the jets. The average Nu sharply decreases with a decrease in S/d.
- The surface motion has a minor effect on the Nu distribution on a moving flat surface for orthogonal jets compared to the angled jets. The average value of the Nu is the highest for the orthogonal jet.
- The pressure force coefficient on a moving flat surface is highly dependent on the H/d and θ but relatively insensitive to the Re, S/d, and VR. Therefore, identification of optimum H/d and θ is very important for products sensitive to pressure forces.
- Two correlations describing the averaged Nu and the pressure force coefficient have been developed. There is a reasonable agreement between the numerical results and the correlation equations.

REFERENCE

[1] Weigand, B., Spring, S. (2011). Multiple jet impingements-a review. Heat Transfer Research, 42: 101-142. https://doi.org/10.1615/HeatTransRes.v42.i2.30

[2] Zuckerman, N., Lior, N. (2006). Jet impingement heat transfer: physics, correlations, and numerical modeling. Advances in Heat Transfer, 39: 565-631. https://doi.org/10.1016/S0065-2717(06)39006-5

[3] Lee, J., Ren, Z., Ligrani, P., Lee, D.H., Fox, M.D., Moon, H.K. (2014). Cross-flow effects on impingement array heat transfer with varying jet-to-target surface distance and hole spacing. International Journal of Heat and Mass Transfer, 75: 534-544. https://doi.org/10.1016/j.ijheatmasstransfer.2014.03.040

[4] Katti, V., Prabhu, S.V. (2009). Influence of streamwise pitch on the local heat transfer characteristics for in-line arrays of circular jets with cross-flow of spent air in one direction. International Journal of Heat and Mass Transfer, 45: 1167-1184. https://doi.org/10.1007/s00231-009-0491-z

[5] San, J.Y., Chen J.J. (2014). Effects of jet-to-jet spacing and jet height on heat transfer characteristics of an impinging jet array. International Journal of Heat and Mass Transfer, 71: 8-17. https://doi.org/10.1016/j.ijheatmasstransfer.2013.11.079

[6] Li, Y., Li, B. (2018). Flow and heat transfer of parallel multiple jets obliquely impinging on a flat surface. Applied Thermal Engineering, 133: 588-603. https://doi.org/10.1016/j.applthermaleng.2018.01.064

[7] Chandramohan, P., Murugesan, S.N., Arivazhagan, S. (2017). Heat transfer analysis of flat plate subjected to multi-jet air impingement using principal component analysis and computational technique. Journal of Applied Fluid Mechanics, 10(1): 293-306. https://doi.org/10.18869/acadpub.jafm.73.238.26337

[8] Li, W., Li, X., Ren, J., Jiang, H., Yang, L., Ligrani, P. (2016). Effect of Reynolds number, hole patterns and hole inclination on cooling performance of an impinging jet array: Part I-convective heat transfer results and optimization. Turbo Expo: Power for Land, Sea, and Air, 49798: V05BT16A003. https://doi.org/10.1115/GT2016-56205

[9] Li, W., Xu, M., Ren, J., Jiang, H. (2017). Experimental investigation of local and average heat transfer coefficients under an inline impinging jet array, including jets with low impingement distance and inclined angle. Journal of Heat Transfer, 139(1): 012201. https://doi.org/10.1115/1.4034165

[10] Ekkad, S., Huang, Y., Han, J.C. (2000). Impingement heat transfer measurements under an array of inclined jets. Journal of Thermophysics and Heat Transfer, 14(2): 286-288. https://doi.org/10.2514/2.6524

[11] Kamal, R.M., El sayed Mostafa, M., Aziz, S.S.A. (2006). An experimental study of an oblique multiple circular air jets impingement on a flat plate. Eight International Congress of Fluid Dynamics and Propulsion, Egypt.

[12] Attala, M., Hussein M., Specht E. (2017). Effect of inclination angle of pair of jets on heat transfer into the flat surface. Experimental Thermal and Fluid Science, 85: 85-94. https://doi.org/10.1016/j.expthermflusci.2017.02.023

[13] Chattopadhyay, H. (2006). Effect of surface motion on transport processes due to circular impinging jets - a numerical study. J. Drying Technology, 24(11): 1347-1351. https://doi.org/10.1080/07373930600951117

[14] Badra, J., Masri, A.R., Behnia, M. (2013). Enhanced transient heat transfer from arrays of jets impinging on a moving plate. Heat Transfer Engineering, 34(4): 361-371. https://doi.org/10.1080/01457632.2013.717046

[15] Kadiyala, P.K., Chattopadhyay, H. (2017). Numerical simulation of transport phenomena due to array of round jets impinging on hot moving surface. Drying Technology, 35(14): 1742-1754. https://doi.org/10.1080/07373937.2016.1275672

[16] Xing, Y., Spring, S., Weigand, B. (2010). Experimental and numerical investigation of heat transfer characteristics of inline and staggered arrays of impinging jets. Journal of Heat Transfer, 132(9): 092201. https://doi.org/10.1115/1.4001633

[17] Wae-hayee, M., Tekasakul, P., Nuntadusit, C. (2013). Influence of nozzle arrangement on flow and heat transfer characteristics of arrays of circular impinging jets. Songklanakarin Journal of Science & Technology, 35(2): 203-212.

[18] Wang, X.K., Niu, G.P., Yuan, S.Q., Zheng, J.X., Tan,

S.K. (2015). Experimental investigation on the mean flow field and impact force of a semi-confined round impinging jet. Fluid Dynamics Research, 47(2): 025501. https://doi.org/10.1088/0169-5983/47/2/025501
[19] Peter, F., Leiner, W., Fiegib, M. (1997). Impinging radial and inline jets: a comparison with regard to heat transfer, wall pressure distribution and pressure loss. Experimental Thermal and Fluid Science, 14: 194-204. https://doi.org/10.1016/S0894-1777(96)00066-0
[20] Suzuki, T., Tsujimoto, K., Shakouchi, T., Ando, T. (2018). DNS of flow and heat transfer characteristics of multiple impinging jets. 21st Australian Fluid Mechanics Conference, Adelaide, Australia.
[21] Draksler, M., Končar, B., Cizelj, L., Ničeno, B. (2017). Large Eddy Simulation of multiple impinging jets in hexagonal configuration–Flow dynamics and heat transfer characteristics. International Journal of Heat and Mass Transfer, 109: 16-27. https://doi.org/10.1016/j.ijheatmasstransfer.2017.01.080
[22] STAR-CCM Documentation. https://www.plm.automation.siemens.com/media/global/en/Siemens%20PLM%20Simcenter%20STAR-CCM_tcm27-62845.pdf.
[23] Roache, P.J. (1994). A method for uniform reporting of grid refinement studies. Journal of Fluids Engineering, 116(3): 405-413. https://doi.org/10.1115/1.2910291

NOMENCLATURE

A	surface area
C_f	force coefficient
d	jet diameter
F	force
H	nozzle-to-surface distance
k	thermal conductivity
Nu	Nusselt number
P	pressure
q	convective heat flux
Re	Reynolds number
S	jet-to-jet spacing
T	temperature
V	= magnitude of jet exit velocity
y^+	dimensionless wall distance

Greek letters

k	turbulence kinetic energy
ω	specific dissipation rate of turbulence kinetic energy
θ	jet exit angle with respect to the horizontal axes, deg
ρ	density of the fluid

Subscripts

ave	average
j	jet
w	wall

Abbreviation

CFD	computational fluid dynamic
GCI	grid convergence index
VR	relative velocity; surface to jet velocity
SST	shear stress transport